
Using Vascular Structure for CT-SPECT Registration in the Pelvis

Russell J. Hamilton, Michael J. Blend, Charles A. Pelizzari, Barrett D. Milliken and Srinivasan Vijayakumar

Department of Radiation and Cellular Oncology, University of Chicago, Chicago; Department of Radiation Oncology, University of Illinois Hospital, Chicago; and Section of Nuclear Medicine, Department of Radiology, University of Illinois Hospital, Chicago, Illinois

The authors outline a method for three-dimensional registration of pelvic CT and ^{111}In -labeled monoclonal antibody capromab pendetide (^{111}In MoAb 7E11.C5) images using $^{99\text{m}}\text{Tc}$ -labeled red blood cell SPECT data. **Methods:** This method of CT-SPECT registration relies on the identification of major blood vessels in the CT and $^{99\text{m}}\text{Tc}$ SPECT images. The vessels are segmented from the image datasets by outlining them on transverse planar slices using a mouse-based drawing tool. Stacking the transverse outlines provides a three-dimensional representation of the vascular structures. Registration is performed by matching the surfaces of the segmented volumes. Dual isotope acquisition of ^{111}In and $^{99\text{m}}\text{Tc}$ activities provides precise SPECT-SPECT registration so that registration in three dimensions of the ^{111}In MoAb and CT images is achieved by applying the same transformation obtained from the $^{99\text{m}}\text{Tc}$ SPECT-CT registration. **Results:** This method provided accurate registration of pelvic structures and significantly improved interpretation of ^{111}In MoAb 7E11.C5 exams. Furthermore, sites of involvement by prostate cancer suggested by the ^{111}In MoAb examination could be interpreted with the bony and soft tissue (nodal) anatomy seen on CT. **Conclusion:** This method is a general clinical tool for the registration of pelvic CT and SPECT imaging data. There are immediate applications in conformal radiation therapy treatment planning for certain prostate cancer patients.

Key Words: conformal radiation therapy; image registration; prostate cancer; prostate imaging; radioimmunotherapy; SPECT-CT registration

J Nucl Med 1999; 40:347–351

Performing SPECT imaging with a new radioisotope-labeled monoclonal antibody, ^{111}In -labeled monoclonal antibody capromab pendetide (^{111}In MoAb 7E11.C5), was shown to significantly improve the detection of early disease spread in prostate cancer patients (1–3). ^{111}In MoAb 7E11.C5 is an IgG1 murine MoAb that reacts with an antigen in prostatic cell cytoplasmic membrane (prostate specific membrane antigen [PSMA]) but not prostatic specific antigen (PSA) nor prostatic acid phosphatase (PAP). SPECT imaging with ^{111}In MoAb 7E11.C5 gained U.S. Food and Drug

Administration (FDA) approval in November 1996 for staging patients with prostate cancer.

^{111}In MoAb 7E11.C5 is concentrated in normal and malignant prostatic tissue and metastatic sites postinjection, but significant concentrations also accumulate in the vascular system, bowel and bone marrow. Thus, interpretation of ^{111}In MoAb 7E11.C5 SPECT images can be difficult. An imaging approach based on a single simultaneous dual-isotope SPECT acquisition of $^{99\text{m}}\text{Tc}$ -labeled red blood cell (RBC) and ^{111}In MoAb 7E11.C5 was reported by nuclear medicine physicians to increase the detection of disease and to be easier to read and interpret (4).

Even with dual-isotope imaging, the anatomical interpretation of pelvic SPECT data can be difficult. In the dual-isotope acquisition method, $^{99\text{m}}\text{Tc}$ -labeled red blood cells (RBCs) provide images of the vascular structures that allow the normal vessel signals to be subtracted out from the ^{111}In MoAb 7E11.C5 images. However, there is also a great deal of bone marrow and bowel activity in the pelvis, with complex distributions. This activity cannot be subtracted out using the RBC examination.

CT images of the pelvis provide an excellent presentation of anatomical structures. The bony and soft tissue structures in the images provide a framework within which the tumor involvement of the prostatic bed, pelvic lymph nodes, seminal vesicles and bladder indicated by the ^{111}In MoAb 7E11.C5 examination can be interpreted. In addition, the bone marrow uptake in the ^{111}In MoAb 7E11.C5 images can be directly compared to the bony structures. We have therefore developed a method to register the three-dimensional SPECT and CT data. The method relies on the identification of major blood vessels in both the CT and $^{99\text{m}}\text{Tc}$ images. Because the $^{99\text{m}}\text{Tc}$ and ^{111}In data are acquired simultaneously, our method also provides a map between ^{111}In MoAb 7E11.C5 and CT images.

MATERIALS AND METHODS

SPECT Imaging Protocol

SPECT images of the pelvis were obtained 5 d after injection of 5–6 mCi ^{111}In 7E11.C5 MoAb. Five d postinfusion was selected as the ideal time for delayed imaging based on a visual evaluation of image target-to-background ratios observed on days 4, 5 and 6 in five patient studies performed before this investigation (MJ Blend,

Received Mar. 6, 1998; accepted Jun. 18, 1998.

For correspondence or reprints contact: Russell J. Hamilton, PhD, Radiation Oncology, University of Illinois Hospital, Suite C-200, M/C 933, 1740 W. Taylor St., Chicago, IL 60612.

unpublished data). Patients were required to take a cathartic (4 L Colyte; Block Drug Co., Jersey City, NJ) during the late afternoon or early evening on day 4 postinfusion. If significant colon activity was seen on planar images on day 5, the imaging was discontinued, and the patient was asked to take another dose of cathartic (2–4 L Colyte) and return for imaging on day 6 postinfusion. On day 5 (or day of delayed imaging), a 3-mL sample of whole blood was initially collected from the patient for RBC labeling using the Ultra-Tag Kit procedure (Mallinckrodt, Inc., St. Louis, MO). During the RBCs labeling procedure, whole-body images and planar images of the chest, abdomen and pelvis were obtained. Then the patient was infused with 15–20 mCi ^{99m}Tc -RBC to assure high counts in the ^{99m}Tc window for our CT-SPECT registration. Thirty min after the infusion of ^{99m}Tc -RBCs, simultaneous dual-isotope SPECT imaging of the pelvis (and abdomen if indicated) was performed.

Whole-body and planar images were obtained with a large-field-of-view (FOV) single rectangular-head gamma camera (SMV America SOPHY DSX, Twinsburg, OH) interfaced with a dedicated computer (4). A medium-energy collimator was used throughout the study and both photopeaks of ^{111}In were used with 15% energy windows. Whole-body images were acquired in a 1024 [times] 1024 matrix with a table imaging speed of 8 cm/min. SPECT pelvis images were obtained using a dedicated triple-head camera system (Picker PRISM 3000 \times P; Picker Corp., Cleveland, Ohio) with an attached UNIX-based computer workstation (Picker Odyssey VP). Fifteen percent windows were used for the two ^{111}In photons and a 10% window was used for the ^{99m}Tc . A narrow window of 10% was chosen for ^{99m}Tc to decrease the contribution of Compton scatter from the ^{111}In photons. Visual inspection suggested that the narrower window increased the signal-to-background ratio for the ^{99m}Tc blood pool images. The raw projection images were acquired on a 128 \times 128 matrix with 40 steps per head and 30 s per stop on day 0 and 50 s per stop on day 5. The resulting data had a voxel size of 1.78 mm³. First-order Chang attenuation correction was then applied to the filtered dataset. Orthogonal images were displayed for visualization purposes. For SPECT images, a low-pass filter was used with an order of 5.0 and a cutoff frequency that ranged from 0.17 to 0.25.

CT Imaging

CT scans of patients were performed as a routine part of their radiation therapy treatment planning (Somatom DRH; Siemens Medical, Hoffman Estates, NJ). Approximately 1 h before the scan, patients drank two 500-mL bottles of a standard oral contrast agent (1.23% iodine solution: 18.1-mL gastroview, 525-mL water). With the patient on the exam couch, approximately 30 mL of the same contrast agent was placed in the rectum using a small tube. During the scan, patients received 150-mL nonionic intravenous contrast (Isovue 300; Bracco Diagnostics Inc., Princeton, NJ). A series of transverse images was obtained with a slice spacing of 4 mm, slice thickness of 4 mm, and a FOV encompassing the external surface of the patient (necessary for proper radiation dose calculations) resulting in 512 \times 512 pixel images with pixel sizes between 0.8 and 1.0 mm.

Registration

The method required segmenting vessels from transverse CT and ^{99m}Tc SPECT images (Figs. 1 and 2). An operator segmented the images at a computer workstation using a mouse-based drawing program. Both the CT and SPECT images were resized to 256 \times 256 pixel images as required for use of the drawing software. The

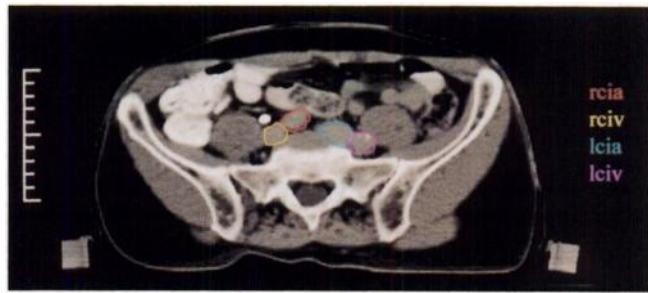


FIGURE 1. Vessels segmented on transverse CT image: right common iliac artery (rcia, red), right common iliac vein (rciv, yellow), left common iliac artery (lcia, cyan), left common iliac vein (lciv, purple).

operator was able to adjust the window and level of the images while segmenting. In addition, the drawing program included an autosegment tool to automatically segment a structure by connecting all pixels having the same value with line segments. Individual arteries and veins were distinguished on CT images. The aorta, inferior vena cava, common iliac, internal iliac and external iliac arteries and veins were delineated. Differentiation between arteries and veins was not possible on the ^{99m}Tc images. Thus, contours were drawn to encompass artery plus vein for each of these same vein/artery pairs on the transverse images. The size of the vessels seen on the ^{99m}Tc SPECT scans depended on the selected viewing threshold. The operator selected a threshold by visually inspecting the images. The autosegment tool was used to delineate the vessels on the SPECT data.

Registration of the ^{99m}Tc SPECT and CT datasets was accomplished by an operator working at a computer workstation using software with a graphical user interface and three-dimensional viewing capabilities to align the SPECT- and CT-defined vascular structures (Fig. 3). The software tool was developed using a commercial software package, AVS (Advanced Visual Systems Inc., Waltham, MA). The tool is similar to a previously described image registration tool (5). The main difference is that a completely manual process, as described later, was used here, because auto-registration did not yield acceptable results for vascular registration.

The operator controlled the registration process completely. Three-dimensional wire ring representations of the ^{99m}Tc and CT structures were displayed in the same viewing window with the operator controlling the viewing angle. The operator moved the SPECT structures with mouse-driven dial gauges or by typing the desired amounts of translations and/or rotations into dialog boxes

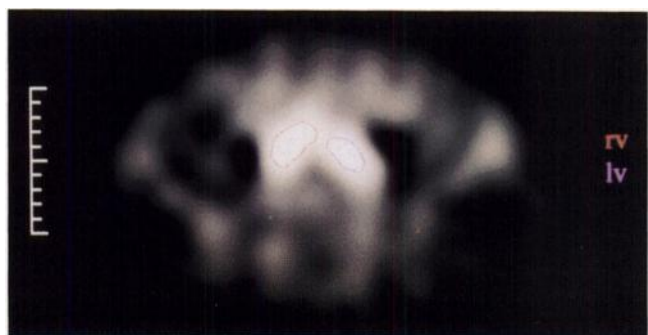


FIGURE 2. Vessels segmented on transverse ^{99m}Tc SPECT image: right common iliac vessels (rciv, red), left common iliac vessels (lciv, purple).

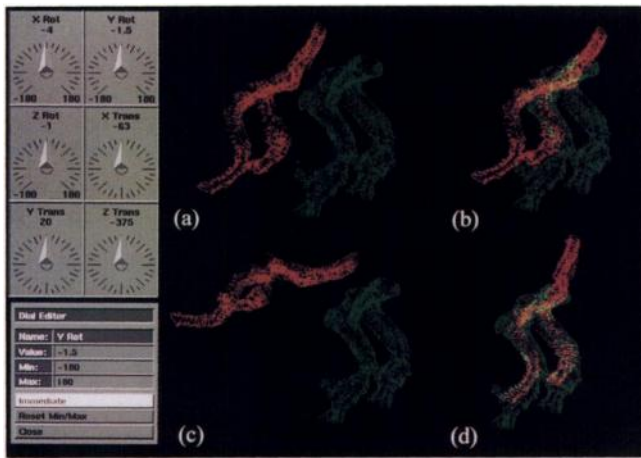


FIGURE 3. Graphical user interface used for registration. Three-dimensional structures of ^{99m}Tc -SPECT (green) and CT (red) segmented vessels are clearly seen. Operator registers CT and SPECT datasets by performing three-dimensional translations and rotations of SPECT-defined structures relative to CT-defined structures until they are aligned. Interface gives operator complete control over registration process. Operator manipulates SPECT image by mouse-driven dial gauges or by typing desired amounts of translations and rotations into dialog boxes. Sequence of frames illustrates process from (a) initial configuration, (b) simple translation, (c) rotation and (d) final alignment.

until they were aligned with the CT structures. All six degrees of freedom of motion were adjusted to achieve the desired alignment. The alignment process typically was performed by aligning the structures from one viewpoint, adjusting the viewpoint, realigning and repeating this process until the structures were aligned from all views. The registration process is well represented by a series of images showing the structures before, during and after the final alignment (Fig. 3). Bifurcations of the vessels were useful for guiding the registration. After the final alignment was achieved, the resulting translations and rotations were used to form a transformation matrix providing a full three-dimensional rigid-body mapping from SPECT to CT (the inverse transformation provided a full three-dimensional rigid-body mapping from CT to SPECT).

The inverse transformation was used to reslice the CT image data along the SPECT imaging planes. The SPECT image pixel intensities were then compared with the resliced CT images by overlaying a color wash of them on the resliced CT images as shown in Figure 4. The accuracy of the registration was verified by examining the areas of high ^{99m}Tc -RBC activity relative to the vessels seen on the CT scan.

The patient orientation was identical for the ^{111}In and ^{99m}Tc scans because of the dual-isotope acquisition method used. Thus, the aforementioned procedure provided registration of ^{111}In and CT, because the transformation between ^{111}In and CT was the same as the transformation between ^{99m}Tc and CT. Finally, the ^{111}In 7E11.C5 MoAb SPECT image pixel intensities were overlaid on the resliced CT images as shown in Figure 5. The regions of increased activity were then interpreted in the context of the known anatomical structures.

Mathematical Description of Transformations

We define ${}_c\mathbf{V}_i = ({}_cX_i, {}_cY_i, {}_cZ_i)$ to be equal to the CT coordinates of the i^{th} surface point of a vascular structure defined by CT and

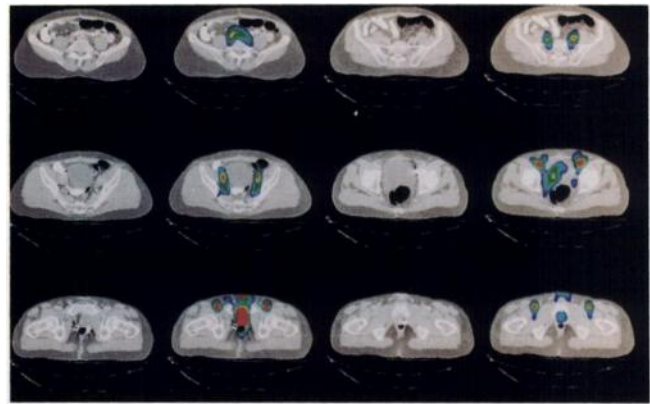


FIGURE 4. Alternating pairs of CT data that have been resliced along transverse SPECT imaging planes according to transformation found from registration process with overlays of ^{99m}Tc -SPECT data on CT images. High (red) to low (blue) levels of SPECT activity are indicated by red to blue color map, respectively.

${}_s\mathbf{V}_i = ({}_sX_i, {}_sY_i, {}_sZ_i)$ to be equal to the SPECT coordinates of the same point. Ideally, a translation vector, \mathbf{T} , and a 3×3 rotation matrix, \mathbf{R} , could be found such that the transformed CT coordinates of all of the surface points would be identical to the SPECT coordinates after applying the translation and rotation to the CT coordinates. If this were possible, the relation

$${}_s\mathbf{V}_i = ({}_c\mathbf{V}_i + \mathbf{T})\mathbf{R}$$

would hold for all i points. However, segmentation errors prevent finding \mathbf{T} and \mathbf{R} such that this relation holds exactly. Instead, the translation vector \mathbf{T}^* and rotation matrix \mathbf{R}^* that provide the best

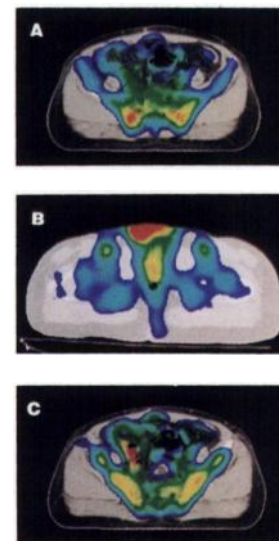


FIGURE 5. Overlays of ^{111}In SPECT data on CT images that have been resliced along transverse SPECT planes according to transformation found from registration process. High (red) to low (blue) levels of SPECT activity are indicated by red to blue color map, respectively. (A) Slice considered to have normal level activity where bone marrow and vascular uptake are well visualized. (B) Slice considered to have disease in central region posterior to pubic bone. (C) Slice considered to have disease before registration but considered to be bowel activity after registration.

fit of the two surfaces is found. An automated method uses the Procrustes algorithm (8,9) to find T^* and R^* by minimizing, σ^2 , the sum of the squares of the distances between the transformed CT points and the SPECT points

$$\sigma^2 = \sum_i (X_i - {}_sX_i)^2 + (Y_i - {}_sY_i)^2 + (Z_i - {}_sZ_i)^2,$$

where ${}_tV_i = (X_i, Y_i, Z_i) = ({}_cV_i + T^*) R^*$ are the coordinates of the transformed CT points. Once T^* and R^* are found, any coordinate point in the CT volume, P_{ct} , is transformed into SPECT volume coordinates, P_s , using the expression

$$P_s = (P_{ct} + T^*)R^*.$$

SPECT coordinate points are transformed into CT volume coordinates using the inverse transformation

$$P_{ct} = (P_s - T^*)R^{*-1},$$

where R^{*-1} is the inverse of R^* .

This automated method has been demonstrated to work well for registration of brain datasets (5). However, we found that it does not provide acceptable results for vascular registration. A manual procedure manipulating the objects using a three-dimensional viewing tool provides good registration of the pelvic vessels. The translation vector T^* and rotation matrix R^* required to align the objects are used to transform any points between the CT and SPECT volumes according to the aforementioned expressions.

RESULTS

SPECT-CT registration was performed on five prostate cancer patients after they had undergone radical prostatectomy. All patients had positive margins and an increasing PSA after surgery; one patient had seminal vesicle involvement. In each case, we found good agreement between the location of ^{99m}Tc -RBC activity and blood vessels in the resliced CT images (Fig. 4). Similarly, regions of high activity found in the ^{111}In images, apart from the abnormal uptake suggestive of prostate cancer cells, matched well with bone marrow in the resliced CT images as expected. Regions of high ^{111}In activity were compared with the anatomy of the resliced CT images to interpret the regions of suspected disease (Fig. 5).

The ^{111}In SPECT-CT registration clarified anatomic structures and provided anatomic localization of regions of high SPECT activity suggestive of disease. The SPECT examinations were first read without CT registration and then were reevaluated after registration. The results are summarized in Table 1. In each case, the SPECT examination was read as positive for disease in the prostatic fossa both before and after registration. Planar and SPECT images alone could not unambiguously determine the locations of increased ^{111}In activity high in the pelvis. Although whole-body planar images clearly demonstrate large bowel activity, small bowel activity is less clearly seen in the SPECT images. In two of the five patients, excessive ^{111}In MoAb uptake high in the pelvis was suspected to be nodal disease before registration but was revealed to be in the small bowel after registration (Fig. 5C).

DISCUSSION

Our motivation to develop a method for registration of ^{111}In MoAb 7E11.C5 SPECT with CT is to enhance radiation therapy treatment of prostate cancer patients postprostatectomy. Recent technological advances provide radiation oncologists the ability to conform their dose prescriptions to a three-dimensional target volume (6). Radiation oncologists obtain volumetric imaging studies (CT or MRI) of their patients and segment the target volumes directly on the digital images at computer workstations using a drawing tool. A treatment plan is constructed by optimizing radiation beam directions and intensities to deliver a tumoricidal dose to the target while not exceeding the dose tolerances of critical structures. The accuracy of dose delivery is on the order of 1–2 mm, which is comparable to the image pixel size. The registration of ^{111}In MoAb 7E11.C5 SPECT with CT will assist in defining the functional and anatomic margins of recurrent or residual disease in the prostatic fossa in patients who had prostatectomies. The ^{111}In MoAb 7E11.C5 SPECT scan identifies areas of gross or microscopic disease that are otherwise invisible. The identified disease can be placed in the anatomical context with the necessary accuracy only by SPECT-CT registration. This procedure might enable radiation oncologists to better conform the radiation dose delivered to these patients. Dose escalation of ^{111}In MoAb 7E11.C5 positive volumes is also made possible by SPECT-CT registration because the geometric relationship between the critical structures, such as rectum and bladder, and the regions of high SPECT activity are clearly demonstrated. Thus, dose may be increased to ^{111}In MoAb 7E11.C5 positive volumes while sparing the critical structures.

The use of vascular structure to register CT with SPECT in the pelvis has been shown to work well. A detailed study of the accuracy of this registration method is beyond the scope of this paper and was not performed. Instead, the ^{99m}Tc images were overlaid on the resliced CT images and the proximity of the regions of high ^{99m}Tc activity with the vessels seen on CT were examined. The areas of high ^{99m}Tc activity corresponded with the vessels within a distance on the order of the reconstructed pixel sizes. The accuracy of this registration method is operator dependent. Registration

TABLE 1
Patient Data with Positive (+) and Negative (–) Findings

Patient	Pathology findings			Initial SPECT finding		Finding after registration	
	Margins	Seminal vesicle	Prostatic fossa	Pelvic nodes	Prostatic fossa	Pelvic nodes	
1	+	–	+	—	+	—	
2	+	+	+	Right iliac	+	Bowel uptake	
3	+	–	+	—	+	—	
4	+	–	+	Right pelvis	+	Bowel uptake	
5	+	–	+	—	+	—	

accuracy depends most on the ability of the operator to align the surfaces of the vessels and to a lesser degree on the ability of the operator to identify and segment vessels on both the CT and SPECT images. Because the entire surface of each vascular structure is used for alignment, segmenting errors on any particular transverse image are not very significant to the final result. The method is more sensitive to differences in the geometric shapes of the vessels at the time of CT and SPECT imaging. Standard, but different, imaging protocols were used for CT and SPECT data acquisition. Despite these differences, acceptable vascular registration of CT and SPECT was achieved. However, differences in bladder and rectal filling were observed to be significant. A uniform imaging protocol for both CT and SPECT is needed to eliminate these differences.

Our method is quick and easy to implement in a clinical service. The entire registration process, including segmenting, takes approximately 2 h once the digital data are transferred to the workstation. An experienced professional staff member, such as a radiation therapy dosimetrist, could be trained to use our software in 4 h. A different approach to register CT with SPECT in the pelvis using bony anatomy was previously described (7). In this method, dual-isotope SPECT acquisition of a bone scintigraph (BS) using ^{99m}Tc hydroxymethylene diphosphonate (HMDP) and an immunoscintigraph using ^{111}In -labeled MoAb were performed on colorectal and ovarian cancer patients. The colorectal cancer patients were given an ^{111}In -labeled carcinoembryonic antigen-specific MoAb whereas the ovarian cancer patients were given ^{111}In -labeled OC125 MoAb. The BS was used to register CT with SPECT in the pelvis. The method required an operator to match two transverse CT slices with the BS from which axial translation and scaling were determined. Next, the operator was required to select a set of homologous points on one or more of the CT and BS slices. The translation, scaling factor and rotation angle in the transverse plane were determined by finding the transformation between the CT and BS defined set of points. This method relies strongly on the ability of the operator to match two particular pairs of transverse images and then to identify a set of homologous points on each image. Errors are expected to arise from the choice of threshold and difficulty in uniquely identifying specific points on SPECT images. This

method assumes that the transverse image planes of the CT are parallel to the transverse imaging planes of the SPECT scan. In addition, the method requires the bony anatomy positions to be the same for both studies. Despite these difficulties and the fact that this method does not provide true three-dimensional registration, the authors found satisfactory results.

CONCLUSION

Our registration method enables full three-dimensional registration of ^{111}In MoAb 7E11.C5 SPECT and CT anatomic data. We expect that our method will improve the detection of the spread of disease in prostate cancer patients by increasing the specificity of ^{111}In MoAb exams. Furthermore, our method can aid radiation oncologists in the treatment of prostate cancer patients postprostatectomy by identifying regions of high ^{111}In MoAb activity in the pelvis. The SPECT-CT registration described here identifies regions of small bowel that may contain ^{111}In MoAb activity, allowing discrimination between this activity and increased pelvic node activity. In the future, this method may be used for image-based dosimetry to guide doses for radioimmunotherapy.

REFERENCES

1. Babaian RJ, Lamki LM. Radioimmunosctigraphy of prostate cancer. *Semin Nucl Med.* 1989;19:309-326.
2. Kahn D, Williams RD, Seldin DW, et al. Radioimmunosctigraphy with ^{111}In labeled CYT-356 for the detection of occult prostate cancer recurrence. *J Urol.* 1994;152:1490-1495.
3. Babaian RJ, Sayer J, Podoloff DA, Steelhammer LC, Bhadkamkar VA, Gulfo JV. Radioimmunosctigraphy of pelvic lymph nodes with ^{111}In labeled monoclonal antibody CYT-356. *J Urol.* 1994;152:1952-1955.
4. Sychra JJ, Lin Q, Blend MJ. The detection of metastatic prostate cancer with simultaneous dual radioisotope SPECT images. *RSNA-EJ* 1997;1.
5. Pelizzari CA, Chen GTY, Spelbring DR, Weichselbaum RR, Chen CT. Accurate three-dimensional registration of CT, PET, and/or MR images of the brain. *J Comput Assisted Tomogr.* 1989;13:20-26.
6. Vijayakumar S, Hellman S. Advances in radiation oncology. *Lancet* 1997;349S2: S111-S113.
7. Liehn J-C, Loboguerrero A, Perault C, Demange L. Superimposition of computed tomography and single photon emission tomography immunoscintigraphic images in the pelvis: validation in patients with colorectal or ovarian carcinoma recurrence. *Eur J Nucl Med.* 1992;19:186-194.
8. Schoeneman PH. A generalized solution of the orthogonal Procrustes problem. *Psychometrika.* 1966;31:1-10.
9. Schoeneman PH, Carroll RM. Fitting one matrix to another under choice of a central dilation and a rigid motion. *Psychometrika.* 1970;35:245-254.